Journal of Advanced Marine Engineering and Technology, Vol. 49, No. 4, pp. 239~244, 2025
J. Advanced Marine Engineering and Technology (JAMET)
https://doi.org/10.5916/jamet.2025.49.4.239

ISSN 2234-7925 (Print)
ISSN 2765-4796 (Online)
Original Paper

Optimization of heat transfer in a vertical cylindrical tube with vertically aligned fins

Eunpil Kim†

(Received July 31, 2025； Revised August 18, 2025；Accepted August 26, 2025)

Abstract: This paper presents the optimal geometric configuration of a passive heat exchanger in a vertical cylinder. The heat exchanger is positioned vertically at the center of the cylinder. Several parameters and flow conditions are investigated to determine the optimal geometric parameters. A finite volume numerical technique is used to obtain computational results. The results showed that the number of fins and the cylinder height imposed a more significant effect as the inlet velocity increased, whereas the fin height showed similar effects for several inlet velocities tested. The best heat flux performance was observed at a fin height of 12 mm and a fin count of 60 at a high inlet velocity. A cylinder length of 240 mm is selected considering geometry restrictions.

Keywords: Finite volume scheme, Forced convection, Heat sink, Channel flow

Nomenclature

c_p	specific heat at constant pressure, $J \cdot kg^{-1} \cdot K^{-1}$
d_{in}	inner diameter of cylinder, mm
d_{out}	outer diameter of cylinder, mm
k	thermal conductivity of fluid, $\boldsymbol{K \cdot m^{-1} \cdot K^{-1}}$
h	height of fin, *mm*
L	total length of cylinder, mm
Nu	average Nusselt number
p	pressure, $\boldsymbol{N \cdot m^{-2}}$
T	fluid temperature, K
V	velocity
x_i	coordinate components, *mm*
v_i	velocity components, $m \cdot s^{-1}$

Greek Symbols

ε	turbulent dissipation rate, $m^2 \cdot s^{-3}$
ρ	density
μ_t	viscous dissipation, $m^2 \cdot s^{-3}$
ν	dynamic viscosity, $kg \cdot s^{-1} \cdot m^{-1}$

Subscripts

∞	ambient
in	inlet
out	outlet

1. Introduction

A plate-fin heat exchanger operates as a passive cooling solution, functioning without the need for external power or active components. Owing to its simple design, it provides high reliability, long operational lifespan, and sustained performance over time. These qualities have made it a widely used technology for many decades.

To improve the efficiency of heat exchangers, the heat transfer rate must be increased, the temperature gap between fluids must be reduced, and the size and weight of the overall system must be minimized. This is typically achieved using extended surfaces, modifying surface structures, or creating secondary flows to disrupt the main flow.

Buyruk *et al.* **[1]** conducted a numerical evaluation of heat transfer enhancement in a plate-fin heat exchanger using a conjugate heat transfer method. They explored the effectiveness of rectangular fins angled at 30° and 90°, positioned with a 10-mm offset from the horizontal axis. E. Kim **[2]** explored natural convection heat transfer in a vertical channel to assess the optimal performance of a plain-fin heat exchanger equipped with two tubes. The study analyzed the flow behavior between isothermal vertical surfaces, focusing on the influence of Rayleigh numbers, plate-fin aspect ratios, and the spacing between the two plates. An *et al.* **[3]** developed an empirical correlation to estimate the

† Corresponding Author (ORCID: http://orcid.org/0000-0002-1679-7961): Professor, Division of Energy Transport Systems Engineering, Pukyong National University , 375, Sinseon-ro, Nam-gu, Busan, 608-739, Korea, E-mail: ekim@pknu.ac.kr, Tel: 051-629-6182

Nusselt number for natural convection from cylinders equipped with vertically aligned plate fins. This correlation was based on a series of comprehensive experiments that examined the effects of varying fin numbers, fin heights, and base surface temperatures. The proposed model was valid within a specific range of Rayleigh numbers and fin-height-to-cylinder-diameter ratios. M. Ganzarolli and C. Alternai **[4]** carried out a study to determine the optimal fin spacing and thickness in the thermal design of a counterflow heat exchanger operating with air. Their approach aimed to minimize the inlet temperature difference and reduce the number of entropy generation units.

Chen *et al*. **[5]** conducted numerical simulations using inverse analysis, the finite difference method, and least-squares techniques. They also provided experimental results to estimate the fin efficiency and average heat transfer coefficient for a plate-fin and single-tube heat exchanger. Zhu and Li **[6]** carried out a numerical investigation of four types of fins including rectangular plate, strip offset, perforated, and wavy fins under laminar flow conditions. Their analysis considered the effects of the fin thickness, thermal entrance region, and end effects within a three-dimensional framework to evaluate the flow and heat transfer characteristics. Kim **[7]** investigated the optimal geometry for a passive heat exchanger placed vertically at the center of a cylindrical enclosure. Various design parameters and flow conditions were examined to identify the most efficient configuration.

The motivation is that small conventional evaporative coolers rely on wet filters that increase the humidity and can lower the cooling efficiency in humid climates. In contrast, the proposed sealed aluminum pipe design uses frozen water bottles to achieve dry cooling, reducing the air temperature without increasing the humidity.

This study explores a vertically oriented plate-fin heat exchanger in which the fins are mounted on the inner wall of an outer cylindrical structure and extend outward from the inner cylinder surface. The system is designed for air cooling in high-temperature environments, suitable for portable cooling applications.

2. Mathematical Modeling

To determine the optimal design parameters for a given geometry, a three-dimensional numerical simulation was conducted. The model features a plate-fin heat exchanger mounted on the inner surface of an outer vertical cylinder, with fins oriented inward toward the central tube. The general domains, as shown in **Figure 1**, were entirely filled with fluid. A fan was positioned at the bottom of the system, creating an upward airflow from bottom to top. **Figure 1(b)** shows the computational fluid domain.

Assuming thin fins, they were positioned vertically and uniformly along the inner circumference of the outer cylinder**. Figure 2** illustrates the complete computational domain of the cylindrical structure. Owing to the high computational cost of simulating the full three-dimensional model, a reduced domain was used based on the rotational symmetry of the system, as shown in **Figure 2(b)**.

To make the simulation more efficient, only a representative sector of the cylinder, focusing on the region where cooling air flows and heat transfer occurs, was analyzed. Symmetry boundary conditions were applied to the radial end faces of the sector. After the simulation, the results from this reduced domain were recalculated to represent the thermal behavior of the entire system.

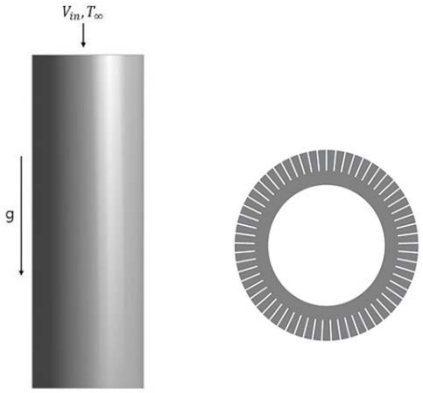

(a) Front view (b) Top view

Figure 1: Schematic illustration of a specified geometry

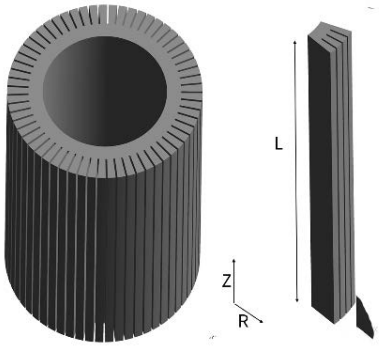

(a) (b)

Figure 2: Computational detailed geometry

For further investigation, the fin configuration and cylinder dimensions of the experimental setup were varied. Although the outer diameter of the outer cylinder remained at 120 mm and the inner pipe diameter at 60 mm, with a consistent fin thickness of 1 mm, several parameters were changed. The number of vertically attached fins on the inner surface of the outer cylinder was adjusted to range from 40 to 68. The fin heights were also explored, increasing from 8 mm to 16 mm. Additionally, the vertical length of the cylinder was modified, with measurements taken between 160 mm and 320 mm.

The simulations were conducted under three-dimensional steady-state conditions with forced convection. To analyze the flow dynamics and heat transfer, the continuity, momentum, and energy equations were applied. Throughout the domain, the fluid properties, including the density, were assumed to remain constant. Turbulence was modeled using the standard k–ε approach, ensuring accurate representation of turbulent flow characteristics.

The following governing equations were used in the analysis.
Continuity Equation:

$$\frac{\partial}{\partial x_i}(\rho u_i) = 0 \tag{1}$$

Momentum Equation:

$$\frac{\partial}{\partial x_j}\left(\rho u_i u_j\right) = -\frac{\partial p}{\partial x_i} + \frac{\partial}{\partial x_j}\left[\mu\left(\frac{\partial u_i}{\partial x_j} + \frac{\partial u_j}{\partial x_i} - \frac{2}{3}\delta_{ij}\frac{\partial u_i}{\partial x_j}\right)\right] + \frac{\partial}{\partial x_j}\left(-\rho\overline{u_\iota' u_j'}\right) \tag{2}$$

Energy Equation:

$$\rho c_p u_i \frac{\partial T}{\partial x_i} = k_c \frac{\partial^2 T}{\partial x_i^2} \tag{3}$$

In these equations, ρ denotes the fluid density, and μ denotes the dynamic viscosity. Variable p represents the pressure, and k_c represents the thermal conductivity. T represents the temperature, and α represents the thermal diffusivity of the fluid. The flow velocity components in the x, y, and z directions are u, v, and w, respectively.

To close the momentum equations, Reynolds stress $-\rho\overline{u_i' u_j'}$ must be modeled. In practice, this is typically achieved using the standard k–ε turbulence model. The associated transport equations for the turbulence variables are as follows:

The turbulence kinetic energy equation:

$$\frac{\partial}{\partial x_i}(\rho k u_i) = \frac{\partial}{\partial x_j}\left[\left(\mu + \frac{\mu_t}{\sigma_k}\right)\frac{\partial k}{\partial x_j}\right] + \mathrm{G}_k + \mathrm{G}_b - \rho\varepsilon - Y_M + z \tag{4}$$

The turbulence rate of dissipation equation:

$$\frac{\partial}{\partial x_i}(\rho\varepsilon u_i) = \frac{\partial}{\partial x_j}\left[\left(\mu + \frac{\mu_t}{\sigma_\varepsilon}\right)\frac{\partial \varepsilon}{\partial x_j}\right] + C_{1\varepsilon}\frac{\varepsilon}{k}(\mathrm{G}_k + C_{3\varepsilon}\mathrm{G}_b) - C_{2\varepsilon}\rho\frac{\varepsilon^2}{k} + S_\varepsilon \tag{5}$$

where G_k is the rate at which turbulent kinetic energy is produced owing to velocity gradients, and G_b signifies the contribution to turbulent kinetic energy arising from buoyancy effects.

$$\mu_t = \rho C_\mu \frac{k^2}{\varepsilon}, \tag{6}$$

where C_μ is a constant.

Model constants are as follows:

$$C_{1\varepsilon} = 1.44;\ C_{2\varepsilon} = 1.92;\ C_\mu = 0.09;\ \sigma_k = 1.0;\ \sigma_\varepsilon = 1.3$$

To assess the thermal performance, the average Nusselt number is determined using the following expression.

$$\overline{Nu} = \frac{\bar{h}L}{k},$$

where $\bar{h}$ is the average heat transfer coefficient, L is the cylinder length, and k is the thermal conductivity.

The numerical analysis was performed using the finite volume method. A second-order upwind scheme was used to discretize both the convective and diffusive terms, and the pressure–velocity coupling was handled using the coupled algorithm. Mesh refinement was applied in regions with strong gradients, particularly near the boundary layers. The simulations were conducted using ANSYS Fluent **[8]** with a constant flow rate specified at the inlet and an ambient pressure set at the outlet. Thermal boundary conditions were applied to the cylindrical surfaces, and the circular end faces of the cylinder were assigned separate conditions.

3. Results and Discussion

This section presents the computational analysis of a heat exchanger that is vertically mounted on the inner surface of an outer cylinder, operating within a forced convection cooling system. The configuration and operating variables of the system were selected to enhance the overall thermal performance. The geometric parameters were selected based on a series of numerical simulations aimed at optimizing the effectiveness of the system. To ensure grid independence, the simulations were performed using multiple mesh densities (see Kim **[7]).**

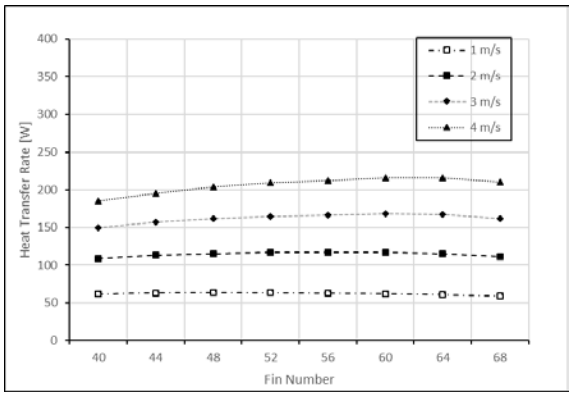

Figure 3: Variations in the heat transfer rate with fin count and inlet velocity changes

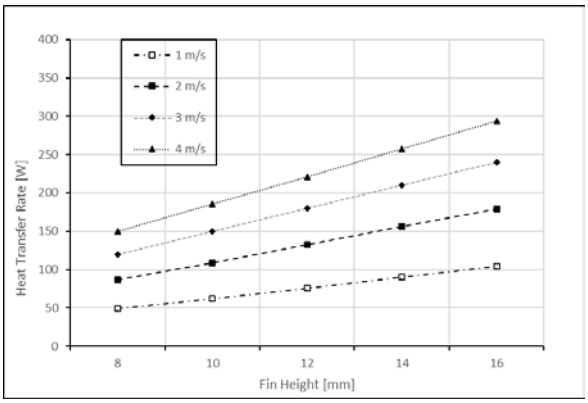

Figure 5: Heat flux variations for different fin heights

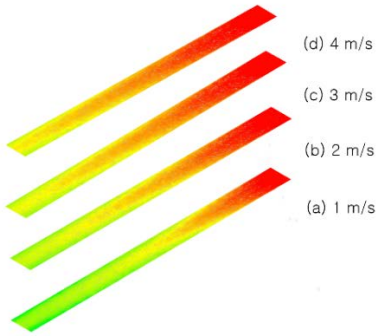

Figure 4: Temperature contours with different inlet velocities

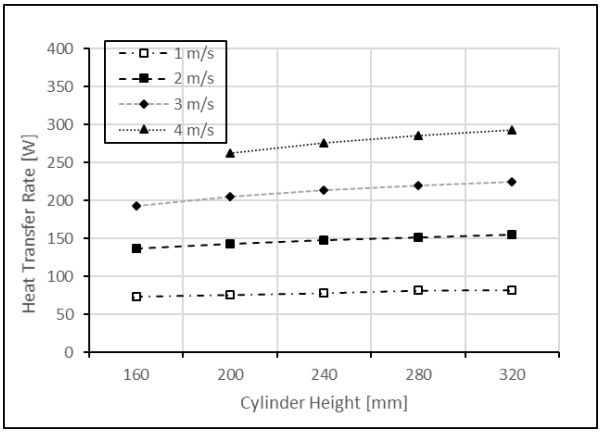

Figure 6: Heat flux variations for different cylinder heights

Figure 3 illustrates the variations in the heat transfer rate as a function of the fin count and inlet velocity at a fixed fin height and cylinder length. In this analysis, the inlet velocity ranged from 1 m/s to 4 m/s, whereas the fin length and cylinder height were fixed at 10 mm and 200 mm, respectively. The number of fins was varied between 40 and 68. As shown in the figure, increasing the number of fins led to an improvement in the heat transfer rate up to approximately 60 fins, after which the rate decreased. This trend was due to the reduction in the fin pitch as more fins were added; this increased the heat transfer surface area but also contributed to a higher flow resistance. At lower inlet velocities, the overall heat transfer was relatively low but improved slightly with increasing velocity. However, beyond a certain point, further velocity increases led to marginal reductions in the heat transfer efficiency. Based on the observed results, a fin count of approximately 60 yielded the most efficient thermal performance under these flow conditions.

As indicated in **Figure 4,** as the inlet velocity increased, the temperature distribution changed accordingly. A noticeable difference was observed between 1 m/s and 2 m/s, whereas a minimal difference was observed between 3 m/s and 4 m/s. This suggested that the heat transfer effect was more significant at lower inlet velocities. However, as the velocity continued to increase, the enhancement in heat transfer became less pronounced because the reduced residence time of the fluid offset the benefits of the stronger convection. As a result, the thermal distribution tended toward uniformity at higher velocities, reflecting diminishing returns in the heat transfer performance.

Figure 5 presents the changes in the heat transfer rate corresponding to various fin heights. In this case, the fins were mounted inwards from the outer surface of the cylinder. Because of the high thermal conductivity of the material, a constant-temperature boundary condition was applied. As illustrated in the figure, increasing the fin height generally led to an increase in the heat transfer rate. The improvement appeared to be nearly linear up to a fin height of approximately 12 mm, demonstrating enhanced thermal performance. This trend remained consistent across different inlet velocities. However, as the inlet velocity increased, the rate at which the heat transfer improved began to decrease. As indicated by the data in **Figure 5**, a fin height of

approximately 12 mm appeared to be optimal under high flow conditions. In contrast, for fin heights of 14 mm and 16 mm, factors such as material costs and modified flow resistance characteristics must also be considered. This indicated that beyond a certain point, further increase in the fin height provided only marginal benefits compared with the additional complexity introduced.

Figure 6 illustrates the heat transfer rates for cylinders with varying heights, positioned vertically within the outer cylinder. The cylinder height ranged from 160 mm to 320 mm in increments of 40 mm. The cylinder heights were selected to ensure a reasonable balance between the confined geometry and system performance. As observed from the graph, the heat transfer rate generally increased with the cylinder height, following a near-linear trend. However, when the inlet velocity was adjusted from 1 m/s to 2 m/s, the heat transfer showed a slight increase compared with the more significant improvements observed at higher inlet velocities of 3 m/s and 4 m/s. Based on the results, notably, further increasing the cylinder height does not substantially contribute to an enhanced performance. Therefore, a cylinder length of 240 mm was selected, considering the geometric constraints.

Figure 7 shows the temperature field contours for different outer wall thermal conditions ranging from 273 K to 293 K. As expected, higher outer wall temperatures resulted in a more uniform and elevated temperature distribution throughout the domain. At the lowest condition of 273 K, a strong temperature gradient was observed near the wall, indicating efficient heat absorption. As the wall temperature increased, the gradient became weaker and the contour colors shifted toward warmer tones, reflecting a reduced driving potential for heat transfer. This demonstrated that the effectiveness of the thermal exchange diminished as the outer wall temperature approached the fluid temperature, leading to a more uniform but less effective cooling performance.

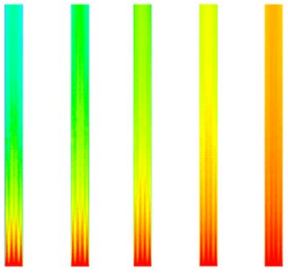

(a) 273 K (b) 278 K (c) 283 K (d) 288 K (e) 293 K

Figure 7: Temperature field contours for a range of outer wall thermal conditions

Table 1: Net heat flux with different outer wall temperatures

	a	b	c	d	e
Outer Wall Temperature [K]	273	278	283	288	293
Net Heat Transfer [W]	17.49	14.25	11.01	7.77	4.53

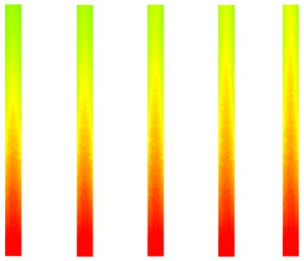

(a) 278 K (b) 283 K (c) 288 K (d) 293 K (e) 298 K

Figure 8: Temperature contours for different inner wall temperatures

Table 1 presents the net heat transfer values corresponding to various outer wall temperatures of the outer cylinder. As the temperature of the outer wall increased from 273 K to 293 K at 5 K intervals, a clear downward trend was observed in the net heat transfer. Specifically, the heat transfer rate decreased from 17.49 W at 273 K to 4.53 W at 293 K. This inverse relationship indicated that a higher external wall temperature reduced the thermal gradient between the inner and outer surfaces, thereby diminishing the overall heat flux. These results demonstrated the significant influence of boundary temperature conditions on the cooling performance of the system.

Figure 8 illustrates the air temperature distribution in response to variations in the internal wall temperature. In this configuration, the temperature of the inner surface was incrementally adjusted from 278 K to 298 K, whereas the temperature of the outer fins on the external cylinder remained constant at 283 K.

The results revealed only minor changes in the thermal profile that could be attributed to the absence of fins on the inner surface. Consequently, the net heat flux exhibited minimal variation throughout the temperature range, indicating that surface geometry played a more significant role than temperature change alone in influencing the heat transfer performance.

4. Conclusions

This study conducted a three-dimensional numerical analysis of a vertical plate-fin heat exchanger within a cylindrical tube under forced convection. The results showed that the fin height, fin count, and cylinder length strongly affected heat transfer, with the optimal

configuration identified as a 12-mm fin height, 60 fins, and a 240-mm cylinder length. These findings reflected the balance between the enhanced surface area and increased flow resistance as well as the diminishing returns of the extended geometry. Compared with surface temperature variations, geometric factors were observed to play the dominant role in the thermal performance. More importantly, the proposed sealed aluminum pipe system offers practical advantages over conventional evaporative coolers by achieving effective dry cooling with frozen water bottles, lowering the air temperature without increasing the humidity, and demonstrating its potential for compact, portable cooling applications.

Acknowledgement

This work was supported by a Research Grant of Pukyong National University (2023 year).

Author Contributions

Conceptualization, E. Kim; Methodology, E. Kim; Software, E. Kim; Formal Analysis, E. Kim; Investigation, E. Kim; Resources, E. Kim; Data Curation E. Kim; Writing-Original Draft Preparation, E. Kim; Writing-Review & Editing, E. Kim; Visualization, E. Kim; Supervision, E. Kim; Project Administration, E. Kim; Funding Acquisition, E. Kim.

References

[1] E. Buyruk, K. Karabulut, and O. Karabulut, “Three-dimensional numerical investigation of heat transfer for plate fin heat exchangers,” Heat Mass Transfer, vol. 49, pp. 817–826, 2013.

[2] E. Kim, “Numerical analysis of a channel flow with two tubes in a vertical plain-fin type heat exchanger,” Journal of the Korean Society of Marine Engineering, vol. 41, no. 5, pp. 383-388, 2017.

[3] B. An, H. J. Kim, and D. Kim, “Nusselt number correlation for natural convection from vertical cylinders with vertically oriented plate fins,” Experimental Thermal and Fluid Science, vol. 41, pp. 59-66, 2012.

[4] M. Ganzarolli and C. Alternai, “Optimum fin spacing and thickness of a finned heat exchanger plate,” Heat Transfer Engineering, vol. 31, pp. 25–32, 2010.

[5] H. -T. Chen, Y. -S. Lin, P. -C. Chen, and J. -R. Chang, “Numerical and experimental study of natural convection heat transfer characteristics for vertical plate fin and tube heat exchangers with various tube diameters,” International Journal of Heat Mass Transfer, vol. 100, pp. 320-331, 2016.

[6] Y. Zhu and Y. Li, “Three-dimensional numerical simulation on the Laminar flow and heat transfer in four basic fins of plate-fin heat exchangers,” Journal of Heat Transfer, vol. 130, no. 11, 2008.

[7] E. Kim, “Heat transfer optimization in a vertical cylinder tube with vertically arranged fins,” Journal of Advanced Marine engineering and Technology, vol. 45, no. 3, pp. 94-99, 2021.

[8] ANSYS Inc. Ver. 16, www.ansys.com, Accessed November 21, 2020.